

EXPERIMENTAL AND OPTIMIZATION DESIGN OF OFFSHORE DRILLING SEAL

Yi Zhang*

Xiaodong Zhang

Xueping Chang

Qian Wu

School of Mechatronic Engineering, Southwest Petroleum University, Chengdu 610500, China

* corresponding author

ABSTRACT

Three-cone bit is the key equipment in the exploration of the oil in offshore drilling and exploration, the bearing system and the seal system are the critical components for the bit. Especially in the offshore drilling environment, the seal design need to be carefully considered. A multi-objective optimization design including orthogonal design method and F-test with finite element analysis for a three-cone bit seal is proposed. Firstly, the calculation method of optimization targets are given, including the minimization of maximum contact pressure and leakage rate analyzed by ANSYS and MATLAB respectively, to maximize seal life and reliability. Then, an orthogonal experiment approach is used to investigate the effects of the eleven parameters on the seal performance, and the influence degrees of the seal factors on the optimization targets have been confirmed by F-test, and the reasonable factors can be determined by the trend of the targets. Finally, in order to validate the analysis results, a new seal was designed and tested on a seal tester compared to the previous seal. In this test, the seal maximum interface temperature that reflects the position of maximum contact pressure can be obtained by using three high precision thermocouples. Both the experiment results and the numerical analyses proved that the maximum contact pressure and leakage rate of the improved seal have been reduced compared to the previous.

Keywords: Offshore drilling; Design Optimization; Seals; Finite Element Analysis; MATLAB

INTRODUCTION

Three-cone bit is the key equipment in the exploration of the oil and natural gas field resources in offshore drilling and exploration. Harsh marine environment brings many problems to drilling, one of the most significant questions which must be answered by the drilling engineers is whether the reliability of three-cone bit can be guaranteed [1]. However, statistics indicated that the main reason for the bit failure is the early seal failure [2].

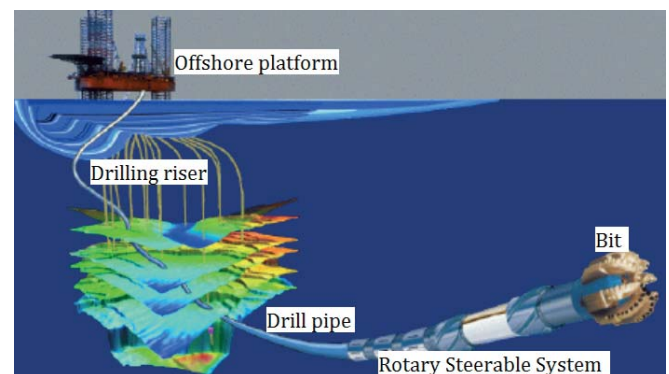


Fig. 1. Schematic diagram of offshore drilling system

Compared to a common seal, the bit seal has more complicated structure, and the high temperature and high pressure of well bottom-hole will lead to the lubricant leakage increases. The statistics identified that the main reason of the bit failure is the early seal failure [3]. The seal fail will lead to the lubricant leakage and fatigue wear caused by the contact pressure of the seal interface [4]. The structure of the SEMS2 is shown in Figure 2: the stator, O-ring, and the rubber support ring are stationary while the rotor rotates together with the shaft. The rubber support ring and the O-ring can supply seal pressure for the seal interface.

In the most recent years, several descriptive studies have been carried out to examine the seal structure and failure reason. Joseph L [5] pointed out that the life of the cone bit bearing is determined by the seal and bearing, and forecasted the life of the lubrication system. Shunhe Xiong [6] produced an axisymmetric numerical model of mechanical seal for down-hole tools, and discussed the relationship between the environmental pressure and the lubricant film. Based on the hypothesis that the drilling fluid has the same fluid properties, a transient seal model and a dynamic tracking model is developed. Considering the seal interface pressure distribution, the second generation SEMS2 has been and improved by Baker Hughes in 2003 [7].

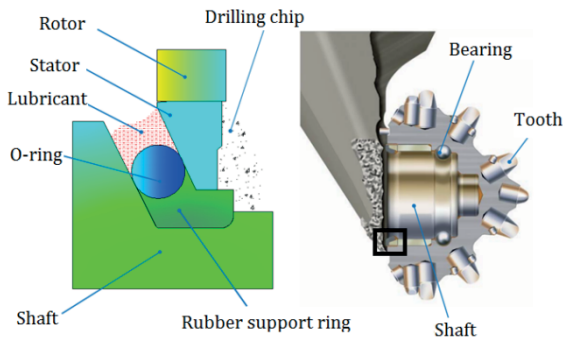


Fig. 2. Seal installation position on the cone bit

As to the bit seal, the sealing force produced by elastomer is non-linear, which further aggravates the research difficulty. Although numerical analysis makes great contributions to the down-hole seal, there still exists some problems for this new seal design. Its seal properties vary with the amount of rubber non-linear behavior, down-hole pressure and seal design parameters. However, very few factors have been considered for the structure optimum design of the cone bit seal nowadays. For the seal optimum design, the artificial neural network [8, 9], Taguchi method [10] and finite element analysis [11] have been recognized as strong tools. However, due to the structure and special environment of the bit seal, the numerical analysis of multiple objectives remains complex.

In this paper, in order to increase the computational efficiency, the inverse method is employed to approximate the pressure distribution of lubricant film by FEM simulation. Furthermore, an orthogonal experiment with orthogonal array and F-test are used to determine the importance of the

seal parameters on the optimum targets. Then the optimal values can be determined by the trend of the average values of maximum contact pressure and leakage rate, and the parameters are verified through numerical analyses and experimental studies.

MATERIAL AND METHODS

MATERIAL PARAMETERS

The material of the head seal and cone insert is hard metal alloy YG8, the backup ring and the head energizer are made of HNBR rubber with a hardness of about 80 IRHD, a material that ensures high temperature resistance together with high compatibility for lubricants, and this material also exhibits highly nonlinear elastic. In this paper, the Mooney–Rivlin model belongs to a type of constitutive models to describe rubber is selected to describe the mechanical properties of rubber with less than 150% deformation. The function of strain potential energy can be expressed as [12]:

$$W = C_1(I_1 - 3) + C_2(I_2 - 3) \quad (1)$$

Where C_1, C_2 are Mooney–Rivlin coefficient, I_1, I_2 are the first and second order invariable strain values. The relationship of stress, strain potential energy, and strain can be expressed as:

$$\sigma = \partial W / \partial \epsilon \quad (2)$$

As to the incompressible materials, shear modulus G and rubber material parameters can be written as:

$$G = 2(C_1 + C_2) \quad (3)$$

The performance parameters C_1 and C_2 can be obtained by uniaxial compression tests, furthermore, the constitutive model parameters of rubber material can be fitted by means of the least square method. According to the fitting results, the constants C_1, C_2 are 1.856 and 0.046 respectively.

CALCULATION METHOD OF OPTIMIZATION TARGETS

SEAL CONTACT PRESSURE

The interface between the stator and the rotor isolates the lubricant from the drilling fluid, and lubricant pressure is higher than drilling fluid by means of the piston balance system, which can prevent the drilling fluid from flowing into the bearings. According to the experimental data, the environmental pressure difference between the lubricant and drilling fluid ranges from 0.3MPa to 0.7MPa [3]. The seal interface contact pressure in downhole condition can be calculated by finite element simulation. The seal assembly

process is first simulated, wherein the shaft is fixed and the axial compressive displacement of stator is 3 mm (Figure 3a). Secondly, the lubricant pressure 30.5 MPa and drilling fluid pressure 30 MPa are exerted on the inside and outside of the seal, respectively, shown in Figure 3b. The result of the contact pressure are depicted in Figure 3c, which shows the outer contact pressure of the interface is smaller than that of the inner at the high pressure environment, and the contact distribution can result in the inner position to be worn easily in the drilling process. Hence, the maximum contact pressure P should be an optimization objective.

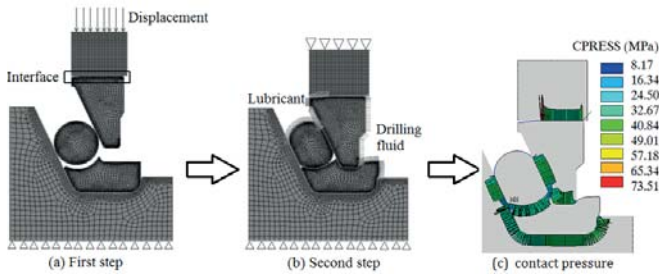


Fig. 3. The steps of the finite element analysis.

SEAL LEAKAGE RATE

The leakage rate is an important index to evaluate the seal life, which can be computed by solving Reynolds equation. Due to the low rotational speed, the inverse method is used to analyze the film thickness of the seal interface to simplify the numerical computation. Due to the axisymmetry of seal geometry and load, the seal surface deformation and flow field of the seal interface can be assumed to be axisymmetric. Based on these hypothesis, the lubrication equation can be expressed as [13]:

$$\frac{1}{r} \frac{\partial}{\partial r} \left(\frac{\phi_r r h^3}{12\mu} \frac{\partial P}{\partial r} \right) = 0 \quad (4)$$

The boundary conditions are: $P=P_1$, at $r=r_0$ (lubricant-side); $P=P_2$, at $r=r_1$ (drilling fluid-side). Where μ represents the dynamic viscosity of the lubricant; P_1 , P_2 , h , r_0 , and r_1 are the lubricant pressure, drilling fluid pressure, film thickness, inner radius of the seal, and the outer radius of the seal, respectively. The leakage rate Q can be calculated from Equation (5):

$$Q = \int_0^{2\pi} \frac{\rho \phi_r r h^3}{12\mu} \frac{\partial p}{\partial r} d\theta \quad (5)$$

The contact pressure gradient distribution of the seal interface can be obtained by finite element simulation. Combined with the Equation (4), the film distribution of the seal interface can be calculated. Based on the film distribution, the seal leakage at the minimum film thickness can be obtained according to the Equation (5).

MULTI-PARAMETER OPTIMIZATION DESIGN

It is obvious that the environmental pressure difference and seal geometric parameters have great influences on the contact pressure and leakage rate. In order to optimize the structural parameters of the seal, the orthogonal design tests and F-tests are used to evaluate the impact degrees on the seal performance.

The seal parameters include environmental pressure difference Δp and ten geometric parameters. The geometric parameters are shown in Figure 4.

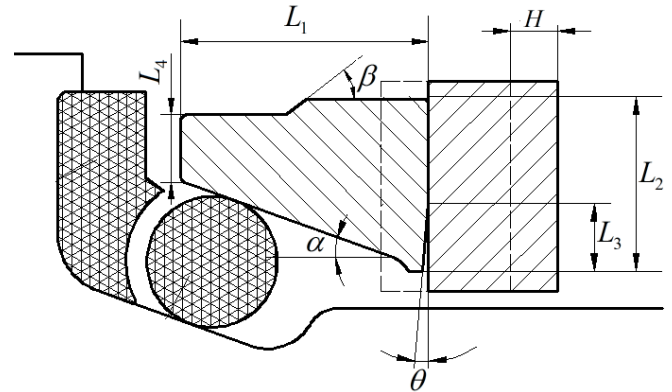


Fig. 4. Parameters of the bearing seal.

The orthogonal design can improve experimental efficiency and has been widely used in industry. In this trial, the factors are labeled as A–M, and each factor has three levels, and the range of each factor has been determined by design experience. The orthogonal design can be conducted by $L_{27}(3^{11})$ Orthogonal Array [14–15]. The levels and factors are given in Table 1.

Tab. 1. Levels and factors of seal parameters

Factors	Parameters	Unit	Levels		
Axial length of the stator(A)	L1	mm	4	5	6
Width of the sealing interface(B)	L2	mm	5	5.5	6
Length of the wedge angle (C)	L3	mm	1	2	3
Inside angle of the stator (D)	α	deg	30	25	20
Outside angle of the stator(E)	β	deg	30	45	60
Wedge angle of the stator (F)	θ	deg	2	5	8
Bottom width of the stator (G)	L4	mm	2	2.5	3
Hardness of the energizer(I)	HA	HIRD	70	80	90
Hardness of the rubber support ring (J)	HB	HIRD	70	80	90
Axial displacement of the rotor(K)	H	mm	1.4	1.6	1.8
Difference of the environmental pressure (M)	ΔP	MPa	0.3	0.5	0.7

RESULTS

MAXIMUM CONTACT PRESSURE AND LEAKAGE RATE

According to the fluid numerical model, the contact pressure gradient distribution can be analyzed by ANSYS. Coupled with the film thickness, the leakage rate Q can be computed by MATLAB. In this paper, the environmental temperature $T=50^\circ$, and the shaft rotating speed $n=200$ r/min. Based on the orthogonal design tests, the maximum contact pressure and the leakage rate are presented in Figure 5. It can be seen that the maximum contact pressure for the 27 trials range from 54.68 MPa to 122.1 MPa; the numbers relatively small are 2, 3, 13, and 14. Meanwhile, the number 2, 3, 13, and 26 trails have relatively larger leakage rate.

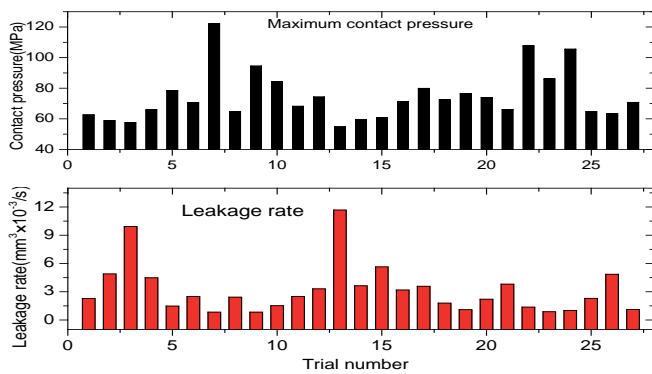


Fig. 5. Maximum contact pressure and leakage rate.

IMPACT FACTORS

According to the results of orthogonal design tests, the variance of the factors can be calculated [16]:

$$S = \frac{1}{a} \sum_{i=1}^b K_i^2 - \frac{1}{n} \left(\sum_{k=1}^n x_k \right)^2 \quad (6)$$

Where,

$$K_i = \sum_{j=1}^a x_j \quad (7)$$

n , a , and b stands for the total number of trials, number of trials for each level, and levels for each factor, x_j is the calculations of the trial j at level i ($i=1, 2, \dots, b; j=1, 2, \dots, a$). The variances of the maximum contact pressure P and leakage rate Q can be seen in Table 2.

Tab. 2. Results of variance analysis of the factors

Variances	Factors										
	A	B	C	D	E	F	G	I	J	K	M
Q	186.55	93.40	36.88	586.5	6.99	13.64	141.92	21.53	96.20	5.35	545.62
P	27.53	17.96	4.26	17.96	5.94	1.59	5.01	35.71	22.46	124	2.21

F-TEST

Based on the orthogonal design and analysis of variance, the influence degree of the factors on the optimization objectives can be confirmed by F-test [17]. The F values of the maximum contact pressure and leakage rate can be calculated by Equation (8):

$$F = \frac{S_i/f_i}{S_E/f_E} \quad (8)$$

Where f_i and f_E are respectively the degrees of freedom of the factor i ($i=A, B, \dots, M$) and of the error; S_i and S_E are the sum of squares of factor i and error respectively. The F-test values can be expressed as the ratio of the variance of the factor i to the variance of the error. In this paper, according to the orthogonal design tests, $n=27$, $a=3$, and the trial number of each factor is 9, so the degrees of freedom $f_i=2, f_E=8$.

The criteria of F values can be found from F distribution table. If $\Phi=0.1$, the confidence level is 90%. For the factors, the larger the F values is, the greater the impact on the optimization objective is. If $F_i > F_{0.001}(2,8)$, the factor i is highly significant, marked as “*****”. If $F_{0.001}(2,8) > F_i > F_{0.005}(2,8)$. The factor i marked as “****”. With the F value increasing from 0.005 to 0.05, the impact on the maximum contact pressure and leakage rate reduces gradually. If $F_{0.05}(2,8) > F_i$, the influence of the factors can be neglected.

According to the criteria, the F values of P and Q for the eleven factors are shown in Table 3. It can be seen that the F values of factors C, E, and F are lower than $F_{0.05}(2,8)$, which means that these factors have little or no effect on P and Q , and the other eight factors need to be further discussed.

Tab. 3. Evaluation results of the factors

Factors	F values										
	A	B	C	D	E	F	G	I	J	K	M
P	9.84	6.42	1.52	6.42	2.12	0.57	1.79	12.77	8.03	44.66	0.79
	***	**	—	**	—	—	—	****	**	*****	—
Q	24.49	12.26	4.84	77.02	0.92	1.79	18.63	2.83	12.63	0.70	71.64
	*****	****	*	*****	—	—	*****	—	****	—	*****

DISCUSSION

OPTIMAL VALUES OF THE OTHER FACTORS

As described above, the influence of the factors C, E, and F can be ignored. For the other eight factors, each factor has nine calculation results on the maximum contact pressure P by the orthogonal array, and so does the leakage rate Q . The average values of P and Q for the same level can be defined as $K-Q$ and $K-P$, then the optimal values can be determined by the trend of the curve of $K-Q$ and $K-P$. Figure 6 presents the trends of $K-P$ and $K-Q$ against the levels for the factors. It can be seen that the factors G and J have great effect on the $K-P$, and the factors B and D have highly effect on the $K-Q$.

In order to extend the seal life, the average values of P and Q need to be reduced as much as possible. According to the trend of $K-P$ and $K-Q$, the level 1, level 1, level 1, and level 3 are chosen as the optimal values for the factors G , J , B , and D .

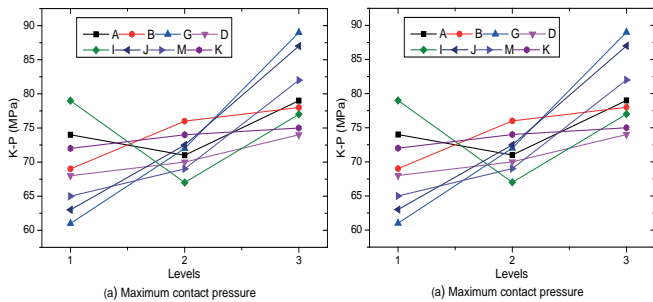


Fig. 6. Average values of the maximum contact pressure and leakage rate.

For the factors A , I , K , and M , Figure 6 shows that the factors I and M have greater impact on the $K-P$ than the $K-Q$, so the $K-P$ should be mainly considered, and the minimum average values for the I and M are level 2 and level 1 respectively, shown in Figure 6(a). By the same reason, the factors A and K have greater impact on the $K-Q$ than the $K-P$, according to Figure 6(b), the level 2, level 2 are considered as the reasonable levels for the seal.

COMPARISON OF SEAL PERFORMANCE

The optimal levels of the seal factors have been obtained through the orthogonal design and F-test, and the comparison of the improved and previous seal is shown in Figure 7. It can be seen that the width of the sealing interface and inner angle of the stator is 4.0mm and 20° versus 5.5 mm and 25° of the previous seal.

Figure 8 shows the contact pressure distributions of improved and previous seal interface. It can be seen that the highest contact pressure is decreased from 73.51MPa to 56.80 MPa, and the middle interface contact pressure distributions are more uniform, which will offer good lubrication environment for the seal. Figure 8 also shows the improved seal increased the outer contact pressure to 55.24MPa versus 48.428MPa for the previous seal, which means that the improved seal can prevent penetration of abrasive particles at the seal outer edge.

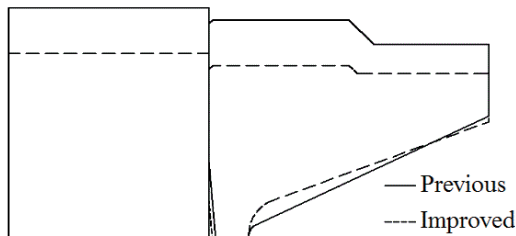


Fig. 7. Seal structure: improved versus the previous.

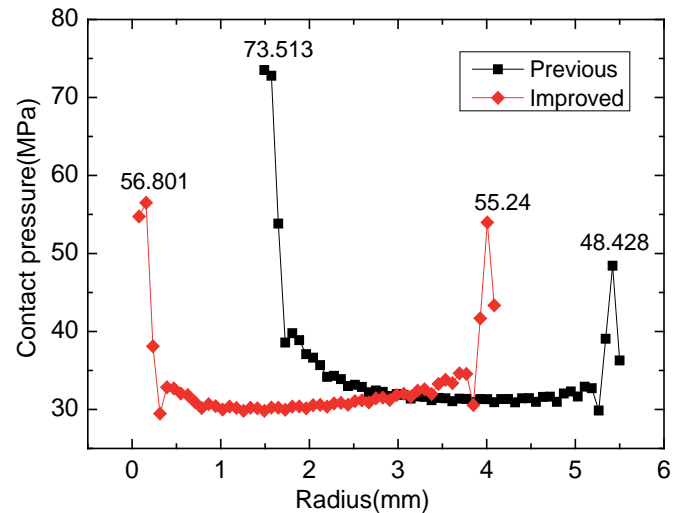


Fig. 8. Comparison of seal contact pressure

SEALING PERFORMANCE TEST

It is difficult to obtain seal contact pressure through experiments. However, the higher contact pressure is the more the friction heat is, so the contact pressure distribution is consistent with temperature distribution, and the interface temperature for the rotor can be measured by three thermocouples at different radius. The seal sample is shown in Fig.8, and the head seal and cone insert are made of stainless steel, after low temperature plasma carburizing, the surface hardness, wear resistance and fatigue capability of stainless steels are largely increased. The schematic of the mechanical seal test rig is shown in Figure 10. The two sides of the cylinder are the lubricant and the water, and an spring in the cylinder can ensure that the lubricant pressure is 0.5 MPa higher than that of the water pressure, the seal leakage can be calculated through the piston area and the piston displacement which can be measured by the displacement sensor.



Fig. 9. Thermocouples installation of the rotor

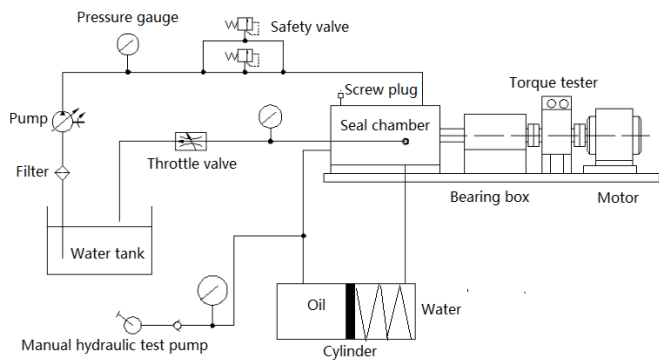


Fig. 10. Schematic of the mechanical seal test rig.

In seal testing, the water pressure is 3MPa. Figure 11 shows that the surface temperature and seal leakage rate rise increases as the seal speed increases. It can be seen that the improved seal temperature is lower than the previous, and both of the trend of the seal leakage rate and the surface temperature are almost the same. When the seal speed reaches 160r/min, the improved seal reduces the temperature to 73° and leakage rate to 2.65 mm³/s versus 76.5° and 3.01 mm³/s for the previous seal.

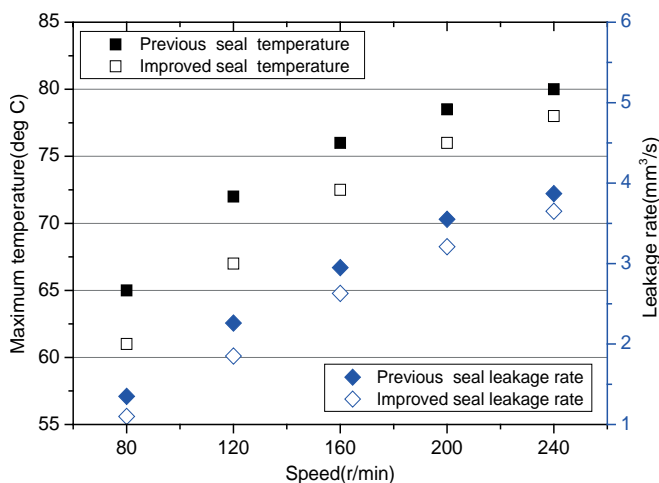


Fig. 11. Comparison of the sealing performance of the test

CONCLUSIONS

This paper has studied the structural optimum design of offshore drilling seal using the numerical simulation and orthogonal design method to extend the sealing life. The contact pressure distribution is obtained by finite element analysis and the pressure gradient distribution is found, then the leakage rate has been computed by MATLAB. The seal parameters are improved after multi-parameter optimization. The numerical analyses and the experiment validate that the maximum contact pressure and leakage rate of the improved seal have been reduced compared to the previous.

(1) On the basis of the fluid mechanics and the numerical method, a new optimization design method of SEMS2 seal has been put forward under the offshore drilling environment.

(2) How to select seal characteristic parameters for decreasing the contact pressure and leakage rate has been analyzed. The result shows that the width of the seal interface, inside angle of the stator, length of the wedge angle, and the bottom width of the stator are important factors and play an important role in the design of the bit seal.

(3) The numerical analyses and experiment validate that the maximum contact pressure and leakage rate for the improved seal have been reduced compared to the previous, thus the optimization method for the bit seal proves to be correct.

(4) Furthermore, the ideal single seal is proposed to have the following characteristics: a more uniform contact pressure distributions to reduce wear and to prolong seal life, and a larger contact pressure on the outer edge to prevent the abrasive particles from coming through.

ACKNOWLEDGEMENTS

This work supported by Research Program supported by the Education Department of Sichuan Province (No.16ZA0062) and the Project of Science and Technology Department of Sichuan Province of China (2014JY0229).

REFERENCES

- Hugo M. Ayala, Douglas P. Hart. 1998. "Wear of elastomeric seal in abrasive slurries." *Wear* 220: 9-21.
- Z Huang, Q Li, Y Zhou, S Jing, et al. 2013. "Experimental research on the surface strengthening technology of roller cone bit bearing based on the failure analysis." *Eng Fail Anal* 29:12-26.
- Y Zhou, Z Huang, L Tan, et al. 2014. "Cone bit bearing seal failure analysis based on the finite element analysis." *Eng Fail Anal* 45: 292-299.
- Joseph L, Kelly Jr. 1990. "Forecasting the Life of Rock Bit Journal Bearings." *SPE* 17565. doi:10.2118/17565-PA.
- Shunhe Xiong, Richard F. Salant. 2000. "A Numerical Model of a Rock Bit Bearing Seal." *Tribology Transactions*. 43 (3): 542-548.
- Tariq A, Mahmoud AH, Tamer W, et al. 2005. "New slim hole technology maximizes productivity in Middle East horizontal drilling programs." *SPE* 92376. doi:10.2118/1105-0058-JPT.
- Karen Bybee. 2006. "Step Change in Performance: Upgraded Bit Technology Improves Drilling Economics." *SPE* 103074. doi:10.2118/1206-0078-JPT.

8. SP Asok, K Sankaranarayanan, T Sundararajan, K Rajesh, GS Ganeshan. 2007. "Neural network and CFD-based optimisation of square cavity and curved cavity static labyrinth seals." *Tribology International* 40(7): 1204-1216.
9. X Ni, Z Zhou, X Wen, L Li. 2011. "The use of Taguchi method to optimize the laser welding of sealing neuro-stimulator." *Optics & Lasers in Engineering* 49(3): 297-304.
10. CT Li, SJ Wu, WL Yu .2014. "Parameter design on the multi-objectives of PEM fuel cell stack using an adaptive neuro-fuzzy inference system and genetic algorithms." *International Journal of Hydrogen Energy* 39(9): 4502-4515.
11. Ping C.Sui, Seth Anderle. 2011. "Optimization of contact pressure profile for performance improvement of a rotary elastomeric seal operating in abrasive drilling environment." *Wear* 271:2466-2470.
12. Beomkeun K, Seong BL, Jayone L, et al. 2012. "A comparison among Neo-Hookean model, Mooney-Rivlin model, and Ogden Model for chloroprene rubber." *Int J Precis Eng Manuf* 13(5):759-764.
13. T Schmidt, M Andre, G Poll. 2010. "A transient 2D-finite-element approach for the simulation of mixed lubrication effects of reciprocating hydraulic rod seals." *Tribology International* 43(10):1775-1785.
14. C Watanabe, A Nagamatsu, C Griffy-Brown. 2003. "Behavior of technology in reducing prices of innovative goods—an analysis of the governing factors of variance of PV module prices." *Technovation* 23(5): 423-436.
15. Xiaohong Jia, Fei Guo, Le Huang, Richard F Salant. 2013. "Parameter analysis of the radial lip seal by orthogonal array method." *Tribology Int* 64:96-102.
16. H.Zhao, G.C.Barber, Q.Zou. 2002. "A study of flank wear in orthogonal cutting with internal cooling." *Wear* 253:957-962.
17. W.H. Yang, Y.S. Tang. 1998. "Design optimization of cutting parameters for turning operations based on the Taguchi method." *J. Mater. Process. Technol* 84:122-129.

CONTACT WITH THE AUTHORS

Yi Zhang

School of Mechatronic Engineering
Southwest Petroleum University
Chengdu 610500
CHINA